IET Microwaves, Antennas & Propagation

Research Article

IET Journals
The Institution of Engineering and Technology

Multiband slot-loaded dipole antenna for WLAN and LTE-A applications

ISSN 1751-8725
Received on 15th January 2017
Revised 15th July 2017
Accepted on 10th September 2017
E-First on 5th December 2017
doi: 10.1049/iet-map.2017.0008
www.ietdl.org

Samir Salem Al-Bawri[1,2], Mohd. Faizal Jamlos[1,3] ✉, Ping Jack Soh[1], Syed Alwee Aljunid Syed Junid[1], Mohd Aminudin Jamlos[1,4], Adam Narbudowicz[5]

[1]*Advanced Communication Engineering Centre (ACE), School of Computer and Communication Engineering, Universiti Malaysia Perlis (UniMAP), 01000 Kangar, Perlis, Malaysia*
[2]*Department of Electronics and Communication Engineering, Faculty of Engineering, Hadhramout University, Al-Mukalla, Yemen*
[3]*Faculty of Mechanical Engineering, Universiti Malaysia Pahang (UMP), 26600 Pekan, Malaysia*
[4]*Department of Electronic, Faculty of Technology Engineering, UniMAP, 02100 Padang Besar, Malaysia*
[5]*Dublin Institute of Technology, Kevin Street, Dublin 8, Ireland*
✉ *E-mail: mohdfaizaljamlos@gmail.com*

Abstract: A multiband printed dipole antenna for wireless local area network (WLAN) and long-term evolution-advanced (LTE-A) applications is investigated here. Its multiband characteristic is enabled by the Y-slot present in the upper arm of the dipole, while the antenna's dimensions are ($0.08\lambda_o \times 0.384\lambda_o$) at the lowest operating frequency. It features bandwidth of 14.6% centred at 2.4 GHz, and ~30.5% centred at 5.5 GHz for WLAN operation. An additional bandwidth of 6.9% centred at 3.5 GHz supporting LTE-A applications is also featured. Besides being compact, the proposed antenna radiates omnidirectionally with a gain of up to 4.09 dBi. Simulations and measurements are in good agreement.

1 Introduction

Wireless communication systems have greatly developed in the past decade, especially for the wireless local area networks (WLANs) and mobile phones. Long-term evolution-advanced (LTE-A) technology has been introduced in commercial, medical, and industrial applications [1, 2]. Both technologies work at different bands of 2, 5, and 3.5 GHz; therefore, a single hardware to cater for operation in all frequency bands is highly desired.

Several examples of multiband WLAN and LTE-A antennas have been previously reported. However, these antennas are relatively large in size. For instance, the printed monopoles featured in [3, 4] are, respectively, sized at ($0.23\lambda_o \times 0.31\lambda_o$) and ($0.28\lambda_o \times 0.20\lambda_o$) with respect to their lowest operating frequency. Gains for the lower, mid, and upper bands are 1.61, 3.39, and 1.78 dBi for [3] and 2.05, 2.6, and 3.55 dBi for [4]. The antenna proposed in [5] featured a 170 mm co-planar waveguide line with a size of $0.033\lambda_o \times 0.516\lambda_o$, with a 2.71 dBi maximum gain. Multiband characteristics were demonstrated in [6] for a planar dipole antenna; however, its performance at higher frequencies (i.e. 5.6 GHz) is very narrowband, with overall size being ($0.46\lambda_o \times 0.08\lambda_o$).

A popular method to miniaturise antennas while enabling multiband operation is by using slots, which allow shifting of resonant modes towards lower frequencies [7–9]. A rectangular slot is used to form the defected ground plane in [10], which enabled wideband operation. Meanwhile, a double L-slot is integrated on a single patch and double patch antenna to realise a triple-band compact antenna operating in the frequency bands of 2.4, 5.2, and 5.8 GHz [11]. Its overall size is ($0.21\lambda_o \times 0.32\lambda_o$). The maximum gains in [12, 13] are, respectively, 1.6 and 2.32 dBi, with lower bandwidth and larger size compared with the proposed antenna. The impedance bandwidths of 17.4, 12.1, and 12.3% are achieved in [14–16], respectively. The gains in [15, 16] are around 3 dBi, whereas in [14], gain as high as 4.8 dBi is reported at the prices of relatively big dimensions. Multiband antennas have also been investigated in [18–20], however with bandwidths at higher frequencies spanning between 13 and 17%, which is less than the proposed antenna.

In this paper, a new compact multiband dipole antenna is proposed for WLAN, with additional support for LTE-A operations at 3.5 GHz. It consists of a printed dipole with a Y-shaped slot tapered in the dipole's body. A net of thin tuning strip is placed around the feed point, which controls input impedance at the upper bands. Besides enabling multiband operation, this technique allows for a compact, low-cost antenna which is realisable in a planar form, using standard printed circuit board etching techniques. To validate this, an overview of double and triple band planar antennas designed for WLAN is presented in Table 1 and compared against the proposed design. It can be seen that for WLAN applications, the proposed antenna features much greater bandwidth than similar antennas with comparable size.

In this paper, a detailed antenna structure and operation mechanism will be first presented, followed by parametric study. Next, results demonstrating reflection coefficients and radiation performance will be analysed and discussed, prior to the concluding remarks.

2 Antenna geometry

Fig. 1 shows the geometry of the proposed dipole antenna. In the upper arm of the dipole, a Y-shaped slot is present, facilitating multiband operation. A second arm without slot forms the lower part of the antenna.

The lack of slot in the lower arm is dictated by a feed cable and its soldering; however, slot in the upper arm is sufficient for proper multiband operation. A net of thin tuning strips with two pairs of symmetric slots (as seen in Fig. 1*b*) is placed around the antenna feed. This creates additional reactance and allows control of two upper bands of the proposed antenna. The fabricated antenna is fed using a 50 Ω SMA connector attached to 35 mm long radio guide coaxial cable as depicted in Fig. 1*c*. The inner conductor of the coaxial cable is soldered to the antenna centre, while its braided outer conductor is soldered to the lower arm of the dipole over a distance of 2 mm. Since the outer cable shield and ground plane are aligned and connected, any common current is expected to interact with the ground plane and contributes to the radiation performance.

Table 1 Comparison of various multiband antennas with the proposed one

Ref.	Antenna type	Dimensions ($W \times L$)	Operating bands		WLAN bandwidth, %	Max gain, dBi
			WLAN, GHz	LTE-A, GHz		
[12]	dipole	$(0.26\lambda_o \times 0.26\lambda_o)$	2.4	—	11	1.69
[13]	dipole	$(0.32\lambda_o \times 0.32\lambda_o)$	5.8	3.5	9.7	2.32
[14]	dipole	$(0.56\lambda_o \times 0.63\lambda_o)$	2.4/5.2/5.8	2.5/3.5	22.5/17.4	4.8
[15]	slot	$(0.64\lambda_o \times 0.64\lambda_o)$	2.4/5.8	3.5	4.1/12.1	3.14
[16]	monopole	$(0.32\lambda_o \times 0.36\lambda_o)$	2.4/(5.2/5.8)	5.5/3.5	3.4/(12.3)	3.20
[17]	dipole	$(0.41\lambda_o \times 0.33\lambda_o)$	2.4	—	7.4	4.3
[18]	slot	$(0.29\lambda_o \times 0.24\lambda_o)$	5.6	2.5/3.5	17.3	3.13
[19]	slot	$(0.22\lambda_o \times 0.26\lambda_o)$	2.4/5.2	2.5/3.5	18.6/13.5	5.09
[20]	monopole	$(0.16\lambda_o \times 0.24\lambda_o)$	2.4/ (5.2/5.8)	5.5/3.5	16.3/ (15.6)	3.40
this work	dipole	$(0.08\lambda_o \times 0.38\lambda_o)$	2.4/ (5/5.2/5.8)	2.5/3.5	14.6/30.5	4.09

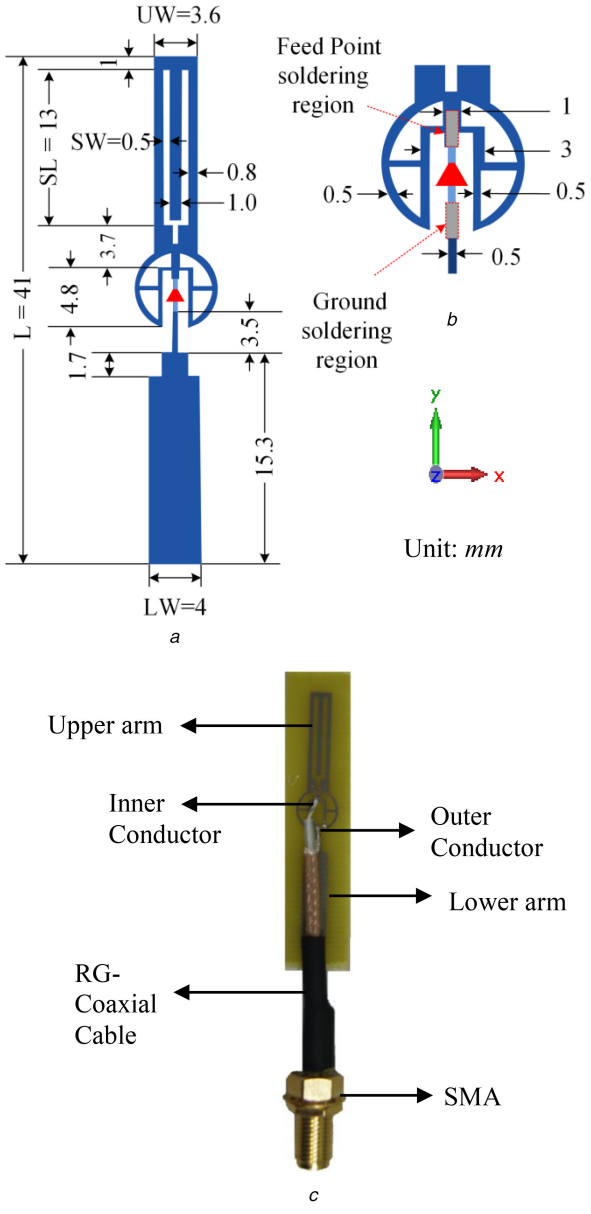

Fig. 1 *Geometry of the proposed antenna*
(a) Whole structure, ***(b)*** Close-up of the tuning strips, ***(c)*** Photograph of the manufactured prototype

This is supposed to prevent common currents on the outer shield and effectively acts as a balun.

The overall size of the proposed antenna is $10 \times 48\,\text{mm}^2$ and it is printed on a low cost, 1.6 mm thick FR4 substrate (with a relative permittivity of 4.3 and loss tangent of 0.025).

3 Working principles

To provide insight into the properties and working principles of the proposed antenna, the simulated current distribution is analysed and discussed. For brevity and clarity, only the upper arm is shown.

3.1 Current distribution

Fig. 2 shows surface current distributions in the upper arm of the dipole at the resonant frequencies of 2.4, 3.5, 5, and 5.8 GHz.

For the lower frequency bands (2.4 and 3.5 GHz), the whole structure exhibits first-order resonance properties at two lower frequencies of 2.4 and 3.5 GHz. The former can be attributed to the overall length of the dipole, which is approximately $\lambda/2$, given the effective permittivity of the antenna milled on FR4 substrate. The latter can be attributed to the Y-shaped slot cut in the dipole's arm. It perturbs the current distribution and therefore creates additional resonance at 3.5 GHz (Fig. 2*b*), producing dipole-like radiation pattern. The length of the slot is 13 mm, which corresponds to the $\lambda/4$, including the effect of effective permittivity due to FR4 substrate. Antenna's operation in the two upper bands of 5 and 5.8 GHz can be attributed to second-order resonant mode, i.e. normally seen for a λ-long dipole with two distinct minima seen for both cases: one at the end of the arm and one around feed point, just above the tuning strips structure.

As will be demonstrated later, the radiation patterns show additional nulls in H-plane – as expected, e.g. from a λ-long dipole. High current concentration around the tuning strips, as seen in Figs. 2*c* and *d*, demonstrate that they fulfil their role to control the resonant frequency for two upper bands.

4 Parametric study

To gain further understanding of the structure, subsequent sections demonstrate the impact of its key parameters.

4.1 Y-shaped slot

The multiband operation of the proposed antenna is mainly achieved by the Y-shaped slot, which is introduced into the upper arm of the dipole. The use of slots to achieve multiband operation has been well described and analysed in the literature [21–23]. It is applied to perturb the current distribution, increase the length of the current path, and generate additional resonances. In the proposed antenna, a new resonance around 3.5 GHz is achieved after optimisation of the Y-shaped slot, when the SL = 13 mm, i.e. $\lambda/4$ at 3.5 GHz when including the effective permittivity of the substrate. The proposed Y-shaped slot perturbs the current distribution, thus creating an additional resonance at 3.5 GHz.

Fig. 3 shows the multiband operation of the proposed antenna without and with different length of Y-slot arms (SL from 5 to 13 mm). For shorter slots, the surface current perturbation is not strong enough and is expected at higher frequencies, where its impact is overshadowed by the two upper resonances. Furthermore, as the Y-slot width (SW) increases, the resonant frequency shifts slightly towards lower frequencies as shown in Fig. 4. When the

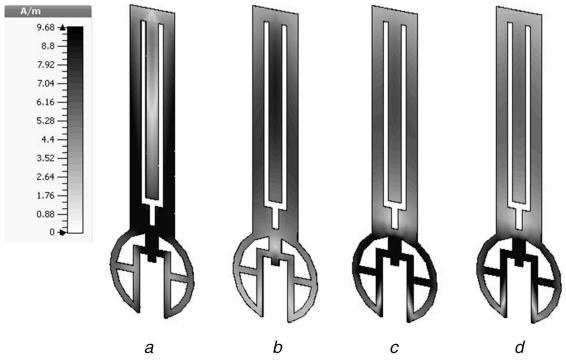

Fig. 2 *Simulated current distribution of the proposed antenna at* ***(a)*** 2.4 GHz, ***(b)*** 3.5 GHz, ***(c)*** 5 GHz, ***(d)*** 5.8 GHz

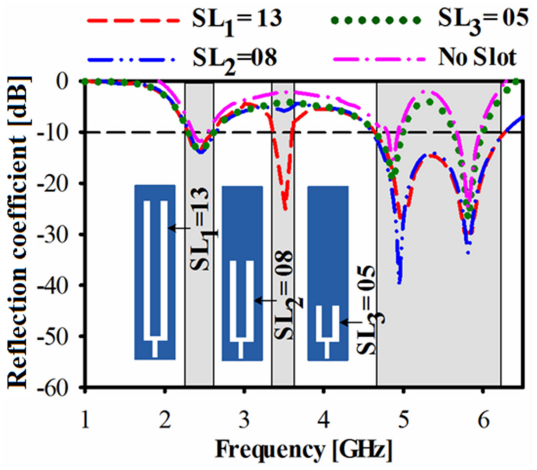

Fig. 3 *Simulated reflection coefficient for different length of Y-slot*

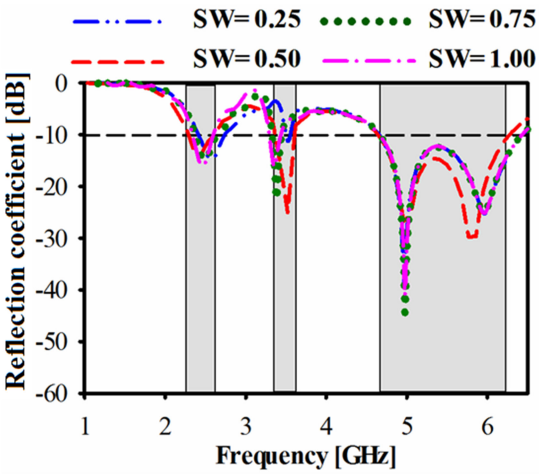

Fig. 4 *Simulated reflection coefficient for different width of Y-slot*

SW is kept very narrow at SW = 0.25 mm and have the same length of SL = 13 mm, it can be observed that the resonance at 3.5 GHz starts to disappear. The optimum values for Y-shaped slot, i.e. SL = 13 mm and SW = 0.5 mm, are chosen to achieve targeted operating frequency bands.

4.2 Net of tuning strips

Figs. 2*c* and *d* show high current concentration in the tuning strips, demonstrating its importance for the upper frequencies. This is further confirmed by a parametric study shown in Fig. 5.

Changing the structure of tuning strips effectively shifts two upper resonances towards lower frequencies. It ensures that both upper resonances create a single, continuous band with good impedance match within wide frequency range (30.5%). It is also seen, that although the resonance at 3.5 GHz is always present, the

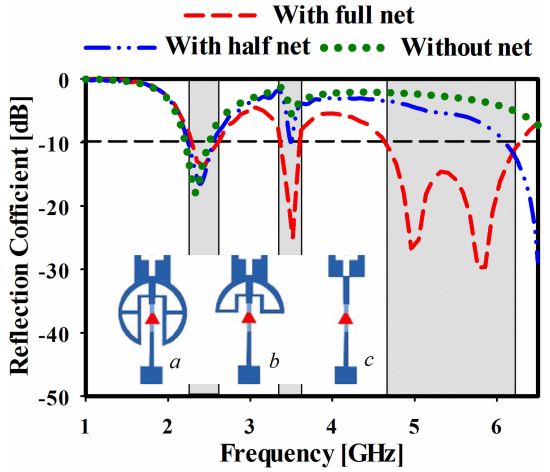

Fig. 5 *Simulated reflection coefficient for ring radiator* ***(a)*** Full net, ***(b)*** Half net, ***(c)*** No net

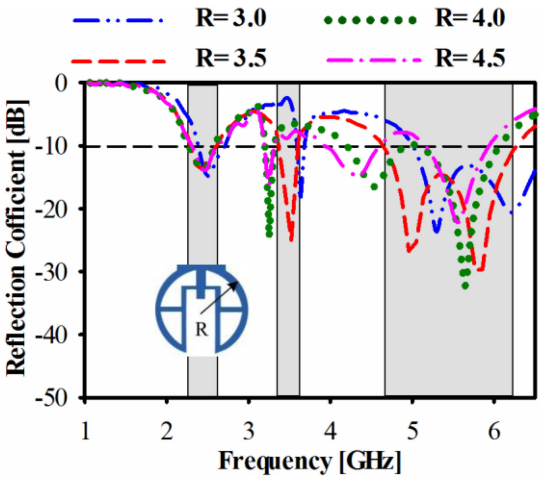

Fig. 6 *Simulated reflection coefficient for net radius R*

tuning strips change its input impedance, facilitating good match. The impact for the lowest band is negligible. In addition, a slight change in the net radiator radius *R* by 0.5 mm in each step can affect the second and the upper resonances frequencies as shown in Fig. 6. It can be observed that both resonances frequencies are shifted strongly towards the lower frequency by increasing the net radius *R*.

Figs. 7*a* and b show the simulated real and imaginary plot, respectively, for the impedance with different variations of net strips in the proposed antenna. The graphs clearly show that when full net of strips is used, the real and imaginary part are close to 50 and 0 Ω at the required resonances frequencies; however, the mismatch in impudence is occurred when there is not strips and half net strips are used, especially at the higher band. This also proves that the net strips are responsible for the frequency tuning at higher band in this antenna.

4.3 Antenna's length L and widths UW and LW

The antenna length (*L*) affects the resonance frequency bandwidth as illustrated in Fig. 8. As expected from theory, longer *L* shifts all bandwidths towards lower frequencies.

The effect of varying dipole's upper and lower arms (UW and LW) is shown in Fig. 9. Both widths are varied together, with the upper arm always 0.4 mm narrower than the lower arm. The effects are most significant for the bandwidth of the middle band at 3.5 GHz.

5 Results and discussion

Prior to the selection and fabrication of a final structure, several important parameters of the proposed antenna are optimised to

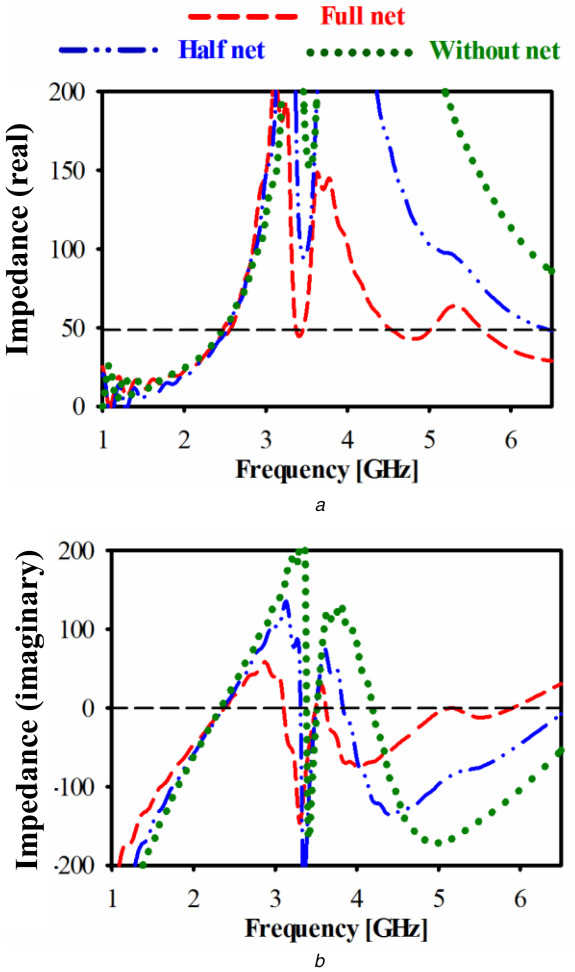

Fig. 7 *Simulated impedance plot of the proposed antenna net*
(a) Real part, ***(b)*** Imaginary part

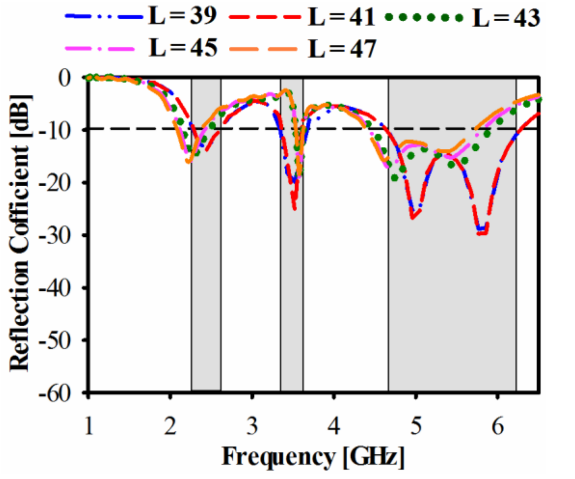

Fig. 8 *Simulated reflection coefficients for different antenna lengths (L)*

Table 2 Summary of the antenna performance

frequency band, GHz	2.4	3.5	5	5.8
gain, dBi	1.89	2.37	4.09	3.86
rad. eff., %	97.5	95.3	92.8	92.4
bandwidth, %	14.6	6.90	30.5	
size, mm		10 × 48	× 1.6	

ensure best performance in terms of multiband operation, bandwidth, and compact size. As was mentioned earlier, the number and width of the target operating bands are determined by dimensions of the Y-shaped slot.

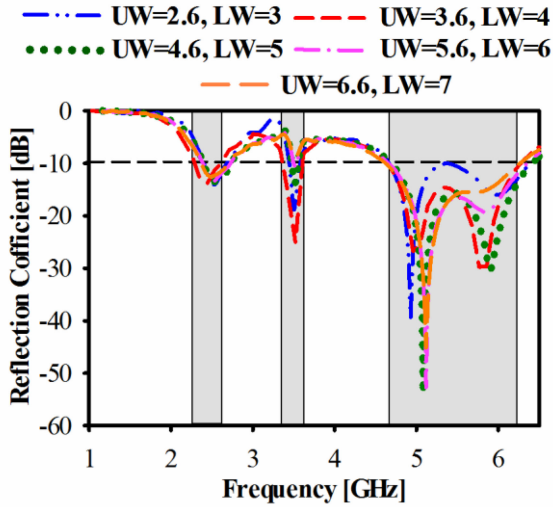

Fig. 9 *Simulated reflection coefficients for different antenna upper and lower arms widths (UW and LW)*

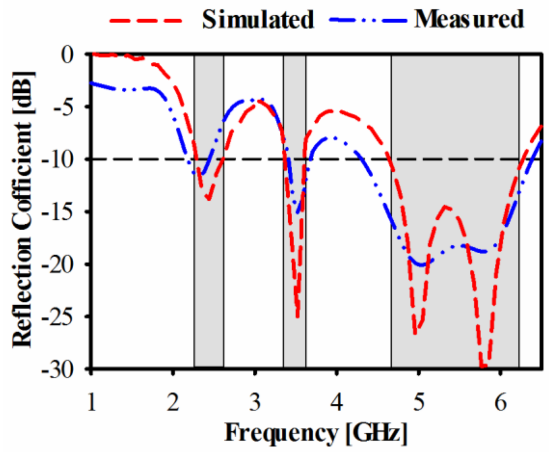

Fig. 10 *Simulated and measured reflection coefficients*

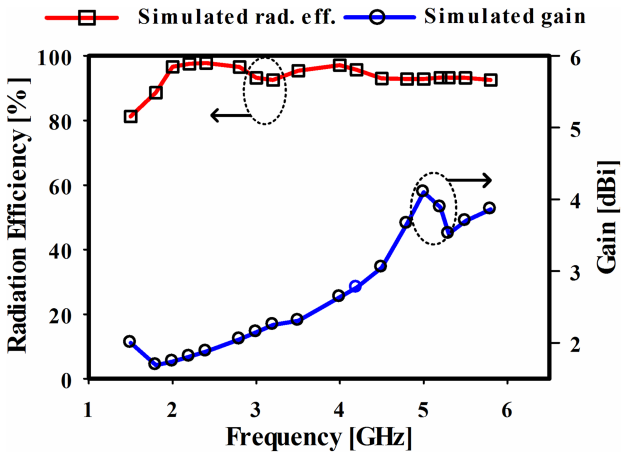

Fig. 11 *Simulated gain and radiation efficiency for the proposed antenna*

It is observed that the increment of slot's length leads to enlarged bandwidths at 2.4 and 5.5 GHz. Fig. 10 demonstrates simulated and measured reflection coefficient of the final prototype. The total final optimised dimensions of the antenna are: $L = 41$ mm, UW = 3.6 mm, LW = 4 mm, SL = 13 mm, SW = 0.5 mm, and $R = 3.5$ mm. The bandwidth of the proposed antenna ranges from a minimum of 240 MHz (from 3.34 to 3.58 GHz, i.e. 6.9%) to a maximum of 1.67 GHz (from 4.64 to 6.31 GHz, i.e. 30.5%). The gain, bandwidth, radiation efficiency (rad. eff.), and the overall size of the multiband antenna are summarised in Table 2 for each frequency.

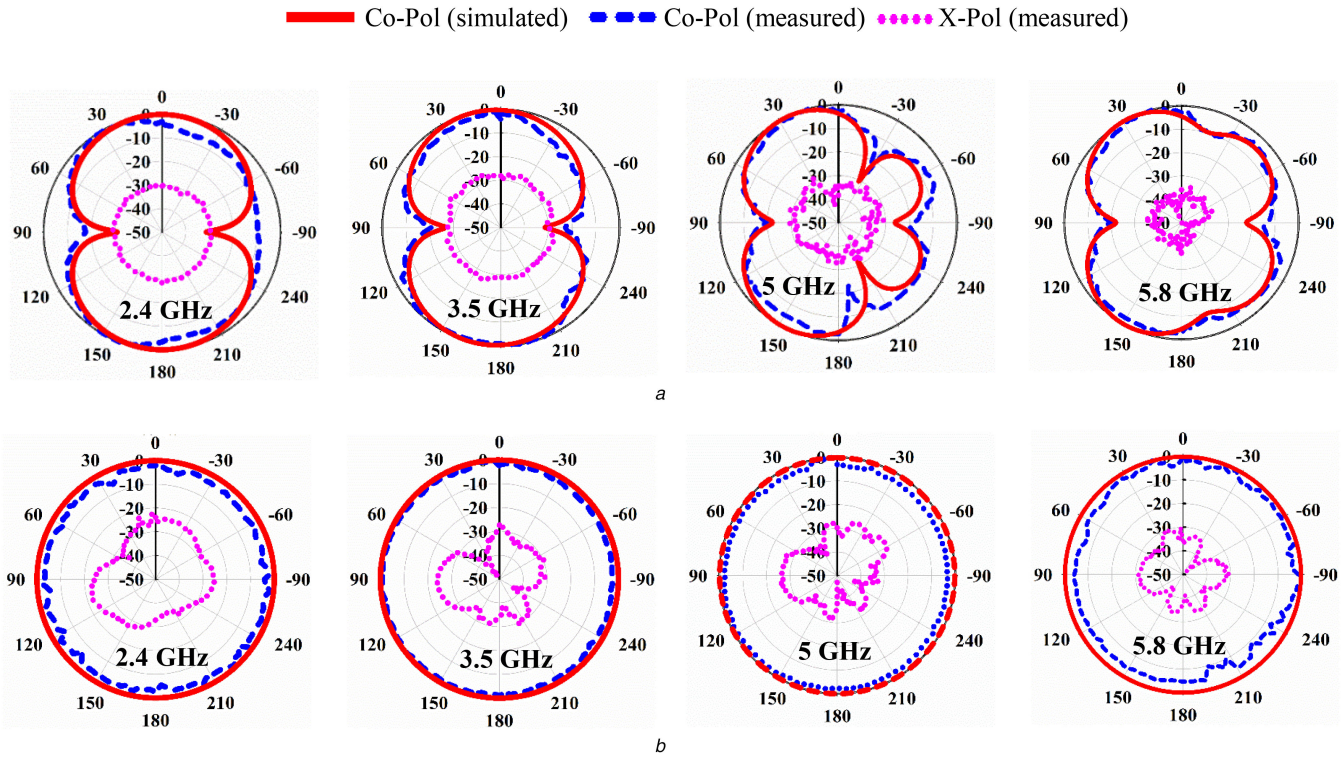

Fig. 12 *Normalised radiation patterns at 2.4, 3.5, 5, and 5.8 GHz*
(a) E-plane, ***(b)*** H-plane

Simulated gain and radiation efficiency variation with respect to the frequency is presented in Fig. 11.

The simulated and measured radiation patterns at 2.4, 3.5, 5, and 5.8 GHz in the azimuth plane are shown in Fig. 12. The antenna radiates vertical polarisation with low levels of cross-polarisations for all bands in the H-plane (*xz*-plane). In the E-plane (*yz*-plane), the proposed antenna features a figure-of-eight shaped radiation pattern for the two lowest bands.

For the two upper bands (Figs. 12*c* and *d*), additional minima can be seen, which are due to the antenna operating in second-order resonant mode (effectively providing similar performance to a λ-long dipole).

There is also a slight discrepancy between simulations and measurements, which is due to the fact that the 35 mm long feed cable is considered as a part of the antenna in measurement but not in the simulation.

6 Conclusion

In this paper, a miniaturised, compact, multiband antenna with broad WLAN bandwidth is proposed. It operates in frequency bands around 2.4, 3.5, and 5.0–5.8 GHz, providing, respectively, 14.6, 6.9, and 30.5% bandwidths. The bands can be tuned by varying length of the Y-slot and a net of tuning strips placed around feed. The slot also contributes to antenna's miniaturisation, yielding its compact size of 10×48 mm^2. The simulated and measured results indicate satisfactory operation with an omnidirectional radiation patterns. With this performance, the low-profile proposed antenna will be suitable candidate for future WLAN applications (5G Wi-Fi) at 5.15–5.875 GHz [24], which also require back-up support of LTE-A network in 3.5 GHz bandwidth.

7 References

[1] Mehdipour, A., Sebak, A.-R., Trueman, C.W., *et al.*: 'Compact multiband planar antenna for 2.4/3.5/5.2/5.8-GHz wireless applications', *IEEE Antennas Wirel. Propag. Lett.*, 2012, **11**, pp. 144–147

[2] Mopidevi, H., Rodrigo, D., Kaynar, O., *et al.*: 'Compact and broadband antenna for LTE and public safety applications', *IEEE Antennas Wirel. Propag. Lett.*, 2011, **10**, pp. 1224–1227

[3] Verma, S., Kumar, P.: 'Compact triple-band antenna for WiMAX and WLAN applications', *Electron. Lett.*, 2014, **50**, (7), pp. 484–486

[4] Xu, Y., Jiao, Y.C., Luan, Y.C.: 'Compact CPW-fed printed monopole antenna with triple-band characteristics for WLAN/WiMAX applications', *Electron. Lett.*, 2012, **48**, (24), pp. 1519–1520

[5] Chen, I.F., Peng, C.M.: 'Printed broadband monopole antenna for WLAN/WiMAX applications', *IEEE Antennas Wirel. Propag. Lett.*, 2009, **8**, pp. 472–474

[6] Nguyen, V.A., Park, B.Y., Park, S.O., *et al.*: 'A planar dipole for multiband antenna systems with self-balanced impedance', *IEEE Antennas Wirel. Propag. Lett.*, 2014, **13**, pp. 1632–1635

[7] Narbudowicz, A., Bao, X.L., Ammann, M.J.: 'Dual-band omnidirectional circularly polarized antenna', *IEEE Trans. Antennas Propag.*, 2013, **61**, (1), pp. 77–83

[8] Row, J.S., Lin, Y.D.: 'Miniaturized designs of circularly polarized slot antenna', *Microw. Opt. Technol. Lett.*, 2014, **56**, (7), pp. 1522–1526

[9] Sarkar, D., Saurav, K., Srivastava, K.V.: 'Multi-band microstrip-fed slot antenna loaded with split-ring resonator', *Electron. Lett.*, 2014, **50**, (21), pp. 1498–1500

[10] Gautam, A.K., Bisht, A., Kanaujia, B.K.: 'A wideband antenna with defected ground plane for WLAN/WiMAX applications', *AEU-Int. J. Electron. Commun.*, 2016, **70**, (3), pp. 354–358

[11] Chitra, R.J., Nagarajan, V.: 'Double L-slot microstrip patch antenna array for WiMAX and WLAN applications', *Comput. Electr. Eng.*, 2013, **39**, (3), pp. 1026–1041

[12] Pan, G., Li, Y., Zhang, Z., *et al.*: 'Isotropic radiation from a compact planar antenna using two crossed dipoles', *IEEE Antennas Wirel. Propag. Lett.*, 2012, **11**, pp. 1338–1341

[13] Boukarkar, A., Lin, X.Q., Jiang, Y.: 'A dual-band frequency-tunable magnetic dipole antenna for WiMAX/WLAN applications', *IEEE Antennas Wirel. Propag. Lett.*, 2016, **15**, pp. 492–495

[14] Si, L.M., Zhang, Q.L., Hu, W.D., *et al.*: 'A uniplanar triple-band dipole antenna using complementary capacitively loaded loop', *IEEE Antennas Wirel. Propag. Lett.*, 2015, **14**, pp. 743–746

[15] Saghati, A.P., Azarmanesh, M., Zaker, R.: 'A novel switchable single-and multifrequency triple-slot antenna for 2.4-GHz bluetooth, 3.5-GHz WiMax, and 5.8-GHz WLAN', *IEEE Antennas Wirel. Propag. Lett.*, 2010, **9**, pp. 534–537

[16] Huang, H., Liu, Y., Zhang, S., *et al.*: 'Multiband metamaterial-loaded monopole antenna for WLAN/WiMAX applications', *IEEE Antennas Wirel. Propag. Lett.*, 2015, **14**, pp. 662–665

[17] Chan, P.W., Wong, H., Yung, E.K.N.: 'Unidirectional antenna composed of dipole and loop', *Electron. Lett.*, 2007, **43**, (22), pp. 1176–1178

[18] Zhang, X.Q., Jiao, Y.C., Wang, W.H.: 'Compact wide tri-band slot antenna for WLAN/WiMAX applications', *Electron. Lett.*, 2012, **48**, (2), pp. 64–65

[19] Hu, W., Yin, Y.Z., Fei, P., *et al.*: 'Compact triband square-slot antenna with symmetrical L-strips for WLAN/WiMAX applications', *IEEE Antennas Wirel. Propag. Lett.*, 2011, **10**, pp. 462–465

[20] Liu, W.C., Wu, C.M., Dai, Y.: 'Design of triple-frequency microstrip-fed monopole antenna using defected ground structure', *IEEE Trans. Antennas Propag.*, 2011, **59**, (7), pp. 2457–2463

[21] Kunwar, A., Gautam, A.K., Rambabu, K.: 'Design of a compact U-shaped slot triple band antenna for WLAN/WiMAX applications', *AEU-Int. J. Electron. Commun.*, 2017, **71**, pp. 82–88

[22] Verma, S., Ansari, J.: 'Analysis of U-slot loaded truncated corner rectangular microstrip patch antenna for broadband operation', *AEU-Int. J. Electron. Commun.*, 2015, **69**, (10), pp. 1483–1488
[23] Khidre, A., Lee, K.-F., Elsherbeni, A.Z*., et al.*: 'Wide band dual-beam U-slot microstrip antenna', *IEEE Trans. Antennas Propag.*, 2013, **61**, (3), pp. 1415–1418
[24] Lai, H.W., Wong, H.: 'Substrate integrated magneto-electric dipole antenna for 5G Wi-Fi', *IEEE Trans. Antennas Propag.*, 2015, **63**, (2), pp. 870–874